

# Fast parallel solution of fully implicit Runge-Kutta and discontinuous Galerkin in time for numerical PDEs, Part I: the linear setting\*

Ben S. Southworth<sup>†</sup>   Oliver A. Krzysik<sup>‡</sup>   Will Pazner<sup>§</sup>  
Hans De Sterck<sup>¶</sup>

December 23, 2024

## Abstract

Fully implicit Runge-Kutta (IRK) methods have many desirable properties as time integration schemes in terms of accuracy and stability, but are rarely used in practice with numerical PDEs due to the difficulty of solving the stage equations. This paper introduces a theoretical and algorithmic framework for the fast, parallel solution of the systems of equations that arise from IRK methods applied to linear numerical PDEs (without algebraic constraints). This framework also naturally applies to discontinuous Galerkin discretizations in time. The new method can be used with arbitrary existing preconditioners for backward Euler-type time stepping schemes, and is amenable to the use of three-term recursion Krylov methods when the underlying spatial discretization is symmetric. Under quite general assumptions on the spatial discretization that yield stable time integration, the preconditioned operator is proven to have conditioning  $\sim \mathcal{O}(1)$ , with only weak dependence on number of stages/polynomial order; for example, the preconditioned operator for 10th-order Gauss integration has condition number less than two. The new method is demonstrated to be effective on various high-order finite-difference and finite-element discretizations of linear parabolic and hyperbolic problems, demonstrating fast, scalable solution of up to 10th order accuracy. In several cases, the new method can achieve 4th-order accuracy using Gauss integration with roughly half the number of preconditioner applications as required using standard SDIRK techniques.

---

\*BSS was supported by Lawrence Livermore National Laboratory under contract B639443, and as a Nicholas C. Metropolis Fellow under the Laboratory Directed Research and Development program of Los Alamos National Laboratory. OAK acknowledges the support of an Australian Government Research Training Program (RTP) Scholarship.

<sup>†</sup>Theoretical Division, Los Alamos National Laboratory, U.S.A. ([southworth@lanl.gov](mailto:southworth@lanl.gov)), <http://orcid.org/0000-0002-0283-4928>

<sup>‡</sup>School of Mathematics, Monash University, Australia ([oliver.krzysik@monash.edu](mailto:oliver.krzysik@monash.edu)), <https://orcid.org/0000-0001-7880-6512>

<sup>§</sup>Center for Applied Scientific Computing, Lawrence Livermore National Laboratory, U.S.A. ([pazner1@llnl.gov](mailto:pazner1@llnl.gov))

<sup>¶</sup>Department of Applied Mathematics, University of Waterloo, Waterloo, Canada ([hdsterck@uwaterloo.ca](mailto:hdsterck@uwaterloo.ca))

# 1 Introduction

## 1.1 Fully implicit Runge-Kutta

Consider the method-of-lines approach to the numerical solution of linear partial differential equations (PDEs), where we discretize in space and arrive at a system of ordinary differential equations (ODEs) in time,

$$M\mathbf{u}'(t) = \mathcal{L}(t)\mathbf{u} + \mathbf{f}(t) \quad \text{in } (0, T], \quad \mathbf{u}(0) = \mathbf{u}_0,$$

where  $M$  is a mass matrix,  $\mathcal{L}(t) \in \mathbb{R}^{N \times N}$  a discrete linear operator, and  $\mathbf{f}(t)$  a time-dependent forcing function.<sup>1</sup> Then, consider time propagation using an  $s$ -stage Runge-Kutta scheme, characterized by the Butcher tableau

$$\begin{array}{c|c} \mathbf{c}_0 & A_0 \\ \hline & \mathbf{b}_0^T \end{array},$$

with Runge-Kutta matrix  $A_0 = (a_{ij})$ , weight vector  $\mathbf{b}_0^T = (b_1, \dots, b_s)^T$ , and quadrature nodes  $\mathbf{c}_0 = (c_1, \dots, c_s)$ .

Runge-Kutta methods update the solution using a sum over stage vectors,

$$\mathbf{u}_{n+1} = \mathbf{u}_n + \delta t \sum_{i=1}^s b_i \mathbf{k}_i, \quad (1)$$

$$M\mathbf{k}_i = \mathcal{L}(t_n + \delta t c_i) \cdot \left( \mathbf{u}_n + \delta t \sum_{j=1}^s a_{ij} \mathbf{k}_j \right) + \mathbf{f}(t_n + \delta t c_i). \quad (2)$$

The stage vectors  $\{\mathbf{k}_i\}$  can then be expressed as the solution of the block linear system,

$$\left( \begin{bmatrix} M & & \mathbf{0} \\ & \ddots & \\ \mathbf{0} & & M \end{bmatrix} - \delta t \begin{bmatrix} a_{11}\mathcal{L}_1 & \dots & a_{1s}\mathcal{L}_1 \\ \vdots & \ddots & \vdots \\ a_{s1}\mathcal{L}_s & \dots & a_{ss}\mathcal{L}_s \end{bmatrix} \right) \begin{bmatrix} \mathbf{k}_1 \\ \vdots \\ \mathbf{k}_s \end{bmatrix} = \begin{bmatrix} \mathbf{f}_1 \\ \vdots \\ \mathbf{f}_s \end{bmatrix}, \quad (3)$$

where  $\mathcal{L}_i := \mathcal{L}(t_n + \delta t c_i)$  and  $\mathbf{f}_i := \mathbf{f}(t_n + \delta t c_i) + \mathcal{L}(t_n + \delta t c_i)\mathbf{u}_n$ . Primarily this paper focuses on spatial operators  $\mathcal{L}$  that are independent of time; however, some of the results hold for commuting operators, such as those that may arise from, for example, a time-dependent reaction term, so for now we maintain this generality.

The difficulty in fully implicit Runge-Kutta methods (which we will denote IRK) lies in solving the  $Ns \times Ns$  block linear system in (3). This paper focuses on the parallel simulation of numerical PDEs, where  $N$  is typically very large and  $\mathcal{L}$  is highly ill-conditioned. In such cases, direct solution techniques to solve (3) are not a viable option, and fast, parallel iterative methods must be used. However, IRK methods are rarely employed in practice due to the difficulties of solving (3). Even for relatively simple parabolic PDEs where  $-\mathcal{L}$  is symmetric positive definite (SPD), (3) is a large nonsymmetric matrix with significant block coupling. For nonsymmetric matrices  $\mathcal{L}$  that already have variable coupling, traditional iterative methods are even less likely to yield acceptable performance in solving (3).

<sup>1</sup>Note, PDEs with an algebraic constraint, such as the divergence-free constraint in the Stokes equations, instead yield a differential algebraic equation (DAE), which requires separate careful treatment, and is addressed in a companion paper along with nonlinearities [46].

## 1.2 Discontinuous Galerkin in time

Discontinuous Galerkin (DG) in time discretizations of systems of linear ODEs give rise to linear algebraic systems of the form

$$\left( \begin{bmatrix} \delta_{11}M & & \delta_{1s}M \\ & \ddots & \\ \delta_{s1}M & & \delta_{ss}M \end{bmatrix} - \delta t \begin{bmatrix} m_{11}\mathcal{L}_1 & \dots & m_{1s}\mathcal{L}_1 \\ \vdots & \ddots & \vdots \\ m_{s1}\mathcal{L}_s & \dots & m_{ss}\mathcal{L}_s \end{bmatrix} \right) \begin{bmatrix} \mathbf{u}_1 \\ \vdots \\ \mathbf{u}_s \end{bmatrix} = \begin{bmatrix} \mathbf{r}_1 \\ \vdots \\ \mathbf{r}_s \end{bmatrix}. \quad (4)$$

The coefficients  $m_{ij}$  correspond to a temporal mass matrix, the coefficients  $\delta_{ij}$  correspond to a DG weak derivative with upwind numerical flux, and the unknowns  $\mathbf{u}_i$  are the coefficients of the polynomial expansion of the approximate solution (for example, see [1, 25, 29, 44]). Both of the coefficient matrices  $\{m_{ij}\}$  and  $\{\delta_{ij}\}$  are invertible. It can be seen that the algebraic form of the DG in time discretization is closely related to the implicit Runge-Kutta system (3) and, in fact, (4) can be recast in the form of (3) using the invertibility of the matrix  $\{\delta_{ij}\}$ . In particular, the degree- $p$  DG method using  $(p+1)$ -point Radau quadrature, which is exact for polynomials of degree  $2p$ , is equivalent to the Radau IIA collocation method [29], which is used for many of the numerical results in Section 3. Thus, although the remainder of this paper focuses on fully implicit Runge-Kutta, the algorithms developed here can also be applied to DG discretizations in time on fixed slab-based meshes.

## 1.3 Outline

This paper develops fast, parallel preconditioning techniques for the solution of fully implicit Runge-Kutta methods and DG discretizations in time for linear numerical PDEs. First, Section 1.4 provides background on why IRK methods are desirable over the simpler and more commonly used diagonally implicit Runge-Kutta (DIRK) methods, and also provides some historical context for the preconditioners developed in this work. Section 1.5 then briefly discusses stable integration from a method-of-lines perspective and introduces two key elements that will be used throughout the paper.

Section 2 introduces a new method to solve for the IRK update (1) for linear operators  $\mathcal{L}$  that are independent of time. This new method requires the preconditioning of  $s$  real-valued matrices of the form  $\eta M - \delta t \mathcal{L}$  for some  $\eta > 1$ , analogous to the matrices that arise in backward Euler integration, and is easily implemented using existing preconditioners and parallel software libraries. In contrast to other works that have considered the preconditioning of (3), the proposed algorithm here (i) is amenable to short-term Krylov recursion (conjugate gradient (CG)/MINRES) if  $\eta M - \mathcal{L}$  is, and (ii) only operates on the solution, thus not requiring the storage of each stage vector. Theory is developed in Section 2.2 that guarantees  $\mathcal{O}(1)$  conditioning of the preconditioned operator under basic assumptions on stability from Section 1.5, with only weak dependence on the number of stages or polynomial order. For example, the preconditioned operator for 10th-order Gauss integration has condition number less than two.

Numerical results are provided in Section 3, demonstrating the new method for a variety of problems and corresponding preconditioners, including very high-order finite-difference and discontinuous Galerkin spatial discretizations of

advection-diffusion equations, and matrix-free continuous Galerkin discretizations of diffusion equations. The method is shown to be fast and scalable up to 10th-order accuracy in time, effective on fully advective (hyperbolic) problems, and, for multiple examples, can obtain 4th-order accuracy with Gauss integration using roughly half as many preconditioning iterations as needed by standard 4th-order SDIRK schemes.

## 1.4 Motivation and previous work

Diagonally implicit Runge-Kutta methods (DIRK), where  $A_0$  is lower triangular, are commonly used in practice. For such schemes, the solution of (3) using a block substitution algorithm requires only  $s$  linear solves of systems of the form  $M - \delta t a_{ii} \mathcal{L}_i$ . Unfortunately, DIRK schemes suffer from order reduction, where the order of accuracy observed in practice on stiff nonlinear PDEs or DAEs can be limited to  $\approx \min\{p, q + 1\}$  or  $q$ , respectively, for integration order  $p$  and stage-order  $q$  [17, 23]. The stage-order of a DIRK method is at most one (EDIRK methods, with one explicit stage, have a maximum stage order of two) and, thus, even a 6th-order DIRK method may only yield first- or second-order accuracy [9]. In contrast, IRK methods may have arbitrarily high stage order and, thus, formally high-order accuracy on stiff, nonlinear problems, and even index-2 DAEs. Although the focus of this paper is linear PDEs without algebraic constraints, we want to highlight that the theory and framework developed here is fundamental to a companion paper on nonlinear PDEs and DAEs [46]. Furthermore, for less stiff problems, IRK methods can yield accuracy as high as order  $2s$  for an  $s$ -stage method, compared with a maximum of  $s$  or  $s + 1$  for SDIRK methods with reasonable stability properties [17, Section IV.6]. Multistep methods can overcome some of the accuracy constraints of SDIRK methods, but implicit multistep methods cannot be A-stable and greater than order two, which is limiting when considering advection-dominated or hyperbolic problems, where the field-of-values often push up against the imaginary axis. Furthermore, for problems where symplectic integration is desirable for conservation, neither linear multistep nor explicit Runge Kutta methods can be symplectic [18]. Although DIRK methods can be symplectic, they are limited to at most 4th order and, moreover, known methods above second order are impractical due to negative diagonal entries of  $A_0$  (leading to a negative shift rather than positive shift of the spatial discretization) [23]. Thus, even moderate order symplectic integration requires IRK methods.

One simplification for using IRK methods is to assume  $\mathcal{L}_i = \mathcal{L}_j$  for all  $i, j$ , in which case (3) can be expressed in Kronecker product form,

$$(I \otimes M - \delta t A_0 \otimes \mathcal{L}) \mathbf{k} = \mathbf{f}. \quad (5)$$

Such an assumption is natural for linear problems with no time-dependent differential components and, for the most part, covers the type of problems studied in this paper. Many papers have considered the solution of (5), with Butcher [10] and Bickart's [6] being some of the earliest works, which develop ways to transform (5) to a simpler form.<sup>2</sup> There, and in many of the works that fol-

<sup>2</sup>In Kronecker form (5), SIRK methods [35] are also relatively straightforward to solve using existing preconditioning techniques. But, although SIRK methods offer some advantages over DIRK methods, they still lack the favorable stability and accuracy properties of IRK methods [8, 37].

lowed, the goal was to minimize the cost of LU decompositions used to solve (5), typically in the context of ODEs.

For large-scale simulation of PDEs, particularly on modern computing architectures, LU decompositions (or other direct factorizations) are typically not feasible. In this vein, a number of people have considered preconditioning techniques for (5) or approximations to (5) on the nonlinear iteration level or time discretization level. Various block preconditioning/approximation techniques have been studied, primarily for parabolic problems [19, 20, 21, 22, 32, 34, 47], and multigrid methods for IRK and parabolic problems were developed in [26]. New ADI-type preconditioners for IRK methods were developed for parabolic problems in [12] with spectral radius shown to be  $< 1$  under reasonable assumptions, and the method extended to the viscous wave equation in first-order form in [13]. More recently, block ILU preconditioners were successfully applied to a transformed version of (5) in [40] on more difficult nonlinear compressible fluids problems. A handful of works have also studied linear solvers for DG-in-time discretizations, primarily for parabolic problems, including block preconditioning approaches [5, 42, 45], and direct space-time multigrid methods [16]. In fact, some of the principles used in this paper are similar to those used in [5] for space-time DG discretizations of linear parabolic problems, and some of the theory derived therein is generalized to non-parabolic/non-SPD operators in this paper.

Despite many papers considering the efficient solution of IRK/DG-in-time methods, very little has been done in the development and analysis of preconditioning techniques for non-parabolic problems/non-SPD spatial operators, particularly methods that are amenable to combine with existing fast, parallel preconditioners. Addressing each of these challenges for linear PDEs is the focus of this work.

## 1.5 A preconditioning framework and stability

Throughout the paper, we use the reformulation used in, for example, [40], where we can pull an  $A_0 \otimes I$  out of the fully implicit system in (3), yielding the equivalent problem

$$\left( A_0^{-1} \otimes M - \delta t \begin{bmatrix} \mathcal{L}_1 & & \\ & \ddots & \\ & & \mathcal{L}_s \end{bmatrix} \right) (A_0 \otimes I) \begin{bmatrix} \mathbf{k}_1 \\ \vdots \\ \mathbf{k}_s \end{bmatrix} = \begin{bmatrix} \mathbf{f}_1 \\ \vdots \\ \mathbf{f}_s \end{bmatrix}. \quad (6)$$

The off-diagonal block coupling in (6) now consists of mass matrices rather than differential operators, which makes the analysis and solution more tractable. The algorithms developed here depend on the eigenvalues of  $A_0$  and  $A_0^{-1}$ , leading to our first assumption.

**Assumption 1.** *Assume that all eigenvalues of  $A_0$  (and equivalently  $A_0^{-1}$ ) have positive real part.*

Recall that if an IRK method is A-stable, irreducible, and  $A_0$  is invertible (which includes DIRK, Gauss, Radau IIA, and Lobatto IIIC methods, among others), then ?? 1 holds [17]; that is, ?? 1 is straightforward to satisfy in practice.

Stability must be taken into consideration when applying ODE solvers within a method-of-lines approach to numerical PDEs. The Dahlquist test problem

extends naturally to this setting, where we are interested in the stability of the linear operator  $\mathcal{L}$ , for the ODE(s)  $\mathbf{u}'(t) = \mathcal{L}\mathbf{u}$ , with solution  $e^{t\mathcal{L}}\mathbf{u}$ . A necessary condition for stability is that the eigenvalues of  $\mathcal{L}$  lie within distance  $\mathcal{O}(\delta t)$  of the region of stability for the Runge-Kutta scheme of choice (e.g., see [41]). Here we are interested in implicit schemes and, because most implicit Runge-Kutta schemes used in practice are A- or L-stable, an effectively necessary condition for stability is that the real part of eigenvalues of  $\mathcal{L}$  be nonpositive. For normal operators, this requirement ends up being a necessary and sufficient condition for stability.

For non-normal or non-diagonalizable operators, the analysis is more complicated. One of the best known works on the subject is by Reddy and Trefethen [41], where necessary and sufficient conditions for stability are derived as the  $\varepsilon$  pseudo-eigenvalues of  $\mathcal{L}$  being within  $\mathcal{O}(\varepsilon) + \mathcal{O}(\delta t)$  of the stability region as  $\varepsilon, \delta t \rightarrow 0$ . Here we relax this assumption to something that is more tractable to work with by noting that the  $\varepsilon$  pseudo-eigenvalues are contained within the field of values to  $\mathcal{O}(\varepsilon)$  [48, Eq. (17.9)], where the field of values is defined as

$$W(\mathcal{L}) := \{\langle \mathcal{L}\mathbf{x}, \mathbf{x} \rangle : \|\mathbf{x}\| = 1\}. \quad (7)$$

This motivates the following assumption for the analysis done in this paper:

**Assumption 2.** *Let  $\mathcal{L}$  be the linear spatial operator, and assume that  $W(\mathcal{L}) \leq 0$  (that is,  $W(\mathcal{L})$  is a subset of the left half plane (including imaginary axis)).*

It should be noted that the field of values has an additional connection to stability. From [48, Theorem 17.1], we have that  $\|e^{t\mathcal{L}}\| \leq 1$  for all  $t \geq 0$  if and only if  $W(\mathcal{L}) \leq 0$ . This is analogous to the “strong stability” discussed by Leveque [27, Chapter 9.5], as opposed to the weaker (but still sufficient) condition  $\|e^{t\mathcal{L}}\| \leq C$  for all  $t \geq 0$  and some constant  $C$ . In practice, ?? 2 often holds when simulating numerical PDEs, and in Section 2.2, it is proven that ?? 1?? 2 guarantee the methods proposed here yield  $\mathcal{O}(1)$  conditioning of the preconditioned operator. It should also be noted that  $\mathcal{L}$  need not be nonsingular.

## 2 Fast parallel preconditioning

For ease of notation, let us scale both sides of (6) by a block diagonal operator, with diagonal blocks  $M^{-1}$ , and let

$$\widehat{\mathcal{L}}_i := \delta t M^{-1} \mathcal{L}_i,$$

for  $i = 1, \dots, s$ . Now let  $\alpha_{ij}$  denote the  $ij$ -element of  $A_0^{-1}$ .<sup>3</sup> Then, solving (6) can be effectively reduced to inverting the operator

$$\mathcal{M}_s := A_0^{-1} \otimes I - \begin{bmatrix} \widehat{\mathcal{L}}_1 & & \\ & \ddots & \\ & & \widehat{\mathcal{L}}_s \end{bmatrix}$$

<sup>3</sup>Note, there are methods with one explicit stage followed by several fully implicit stages [9]. In such cases,  $A_0$  is not invertible, but the explicit stage can be eliminated from the system (by doing an explicit time step). The remaining operator can then be reformulated as in (6).

$$= \begin{bmatrix} \alpha_{11}I - \widehat{\mathcal{L}}_1 & \alpha_{12}I & \cdots & \alpha_{1s}I \\ \alpha_{21}I & \alpha_{22}I - \widehat{\mathcal{L}}_2 & \cdots & \alpha_{2s}I \\ \vdots & \vdots & \ddots & \vdots \\ \alpha_{s1}I & \cdots & \cdots & \alpha_{ss}I - \widehat{\mathcal{L}}_s \end{bmatrix}. \quad (8)$$

We proceed by deriving a closed form inverse of (8), demonstrating how the Runge-Kutta update in (1) can then be performed directly (without forming and saving each stage vector), and developing a preconditioning strategy to apply this update using existing preconditioners.

## 2.1 An inverse and update for commuting operators

This section introduces a result similar to Bickart's [6], but using a different framework and generalized to hold for commuting operators. We consider  $\mathcal{M}_s$  as a matrix over the commutative ring of linear combinations of  $\{I, \widehat{\mathcal{L}}\}$ , and the determinant and adjugate referred to in Lemma 1 are defined over matrix-valued elements rather than scalars. For the interested reader, see [7] for details on matrices and the corresponding linear algebra when matrix elements are defined over a space of commuting matrices.

**Lemma 1.** *Let  $\alpha_{ij}$  denote the  $(i, j)$ th entry of  $A_0^{-1}$  and assume  $\{\widehat{\mathcal{L}}_i\}_{i=1}^s$  are commuting operators. Define  $\mathcal{M}_s$  as in (8), let  $\det(\mathcal{M}_s)$  be the determinant of  $\mathcal{M}_s$ , and let  $\text{adj}(\mathcal{M}_s)$  be the adjugate of  $\mathcal{M}_s$ . Then,  $\mathcal{M}_s$  is invertible if and only if  $\det(\mathcal{M}_s)$  is invertible, and*

$$\mathcal{M}_s^{-1} = \text{diag}(\det(\mathcal{M}_s)^{-1}) \text{adj}(\mathcal{M}_s).$$

where “diag” indicates a block diagonal matrix, with diagonal blocks in this case given by  $\det(\mathcal{M}_s)^{-1}$ . Now, suppose  $\widehat{\mathcal{L}}_i = \widehat{\mathcal{L}}_j$  for all  $i, j$ , and let  $P_s(x)$  be the characteristic polynomial of  $A_0^{-1}$ . Then,

$$\mathcal{M}_s^{-1} = \text{diag}(P_s(\widehat{\mathcal{L}})^{-1}) \text{adj}(\mathcal{M}_s),$$

*Proof.* Notice in (8) that if  $\widehat{\mathcal{L}}_i$  and  $\widehat{\mathcal{L}}_j$  commute for all  $i, j$ , then  $\mathcal{M}_s$  is a matrix over the commutative ring of linear combinations of  $I$  and  $\{\widehat{\mathcal{L}}_i\}$ . Let  $\text{adj}(\mathcal{M}_s)$  denote the matrix adjugate. A classical result in matrix analysis tells us that

$$\text{adj}(\mathcal{M}_s)\mathcal{M}_s = \mathcal{M}_s\text{adj}(\mathcal{M}_s) = \text{diag}(\det(\mathcal{M}_s))I.$$

Moreover,  $\mathcal{M}_s$  is invertible if and only if the determinant of  $\mathcal{M}_s$  is invertible, in which case  $\mathcal{M}_s^{-1} = \text{diag}(\det(\mathcal{M}_s)^{-1})\text{adj}(\mathcal{M}_s)$  [7, Theorem 2.19 & Corollary 2.21]. For the case of time-independent operators ( $\widehat{\mathcal{L}}_i = \widehat{\mathcal{L}}_j$ ), notice that  $\mathcal{M}_s$  takes the form  $A_0^{-1} - \widehat{\mathcal{L}}I$  over the commutative ring defined above. Analogous to a scalar matrix, the determinant of  $A_0^{-1} - \widehat{\mathcal{L}}I$  is the characteristic polynomial of  $A_0^{-1}$  evaluated at  $\widehat{\mathcal{L}}$ .  $\square$

Returning to (6), we can express the solution for the set of all stage vectors  $\mathbf{k} = [\mathbf{k}_1; \dots; \mathbf{k}_s]$  as

$$\mathbf{k} := \text{diag}(\det(\mathcal{M}_s)^{-1}) (A_0^{-1} \otimes I) \text{adj}(\mathcal{M}_s) \mathbf{f},$$

where  $\mathbf{f} = [\mathbf{f}_1; \dots; \mathbf{f}_s]$  (note that  $A_0 \otimes I$  commutes with  $\text{diag}(\det(\mathcal{M}_s)^{-1})$ ). The Runge-Kutta update is then given by

$$\begin{aligned} \mathbf{u}_{n+1} &= \mathbf{u}_n + \delta t \sum_{i=1}^s b_i \mathbf{k}_i \\ &= \mathbf{u}_n + \delta t \det(\mathcal{M}_s)^{-1} (\mathbf{b}_0^T A_0^{-1} \otimes I) \text{adj}(\mathcal{M}_s) \mathbf{f}. \end{aligned} \quad (9)$$

**Remark 1** (Implementation & complexity). *The adjugate consists of linear combinations of  $I$  and  $\widehat{\mathcal{L}}$ , and an analytical form can be derived for an arbitrary  $s \times s$  matrix, where  $s \sim \mathcal{O}(1)$ . Applying its action requires a set of vector summations and matrix-vector multiplications. In particular, the diagonal elements of  $\text{adj}(\mathcal{M}_s)$  are monic polynomials in  $\widehat{\mathcal{L}}$  of degree  $s - 1$  (or linear combinations of comparable degree if  $\widehat{\mathcal{L}}_i \neq \widehat{\mathcal{L}}_j$ ) and off-diagonal terms are polynomials in  $\widehat{\mathcal{L}}$  of degree  $s - 2$ .*

Returning to (9), we consider two cases. First, if a given Runge-Kutta scheme is stiffly accurate (for example, Radau IIA methods), then  $\mathbf{b}_0^T A_0^{-1} = [0, \dots, 0, 1]$ . This yields the nice simplification that computing the update in (9) only requires applying the last row of  $\text{adj}(\mathcal{M}_s)$  to  $\mathbf{f}$  (in a dot-product sense) and applying  $\det(\mathcal{M}_s)^{-1}$  to the result. From the discussion above regarding the adjugate structure, applying the last row of  $\text{adj}(\mathcal{M}_s)$  requires  $(s - 2)(s - 1) + (s - 1) = (s - 1)^2$  matrix-vector multiplications. Because this only happens once, followed by the linear solve(s), these multiplications are typically of relatively marginal cost.

In the more general case of non-stiffly accurate methods (for example, Gauss methods), one can obtain an analytical form for  $(\mathbf{b}_0^T A_0^{-1} \otimes I) \text{adj}(\mathcal{M}_s)$ . Each element in this block  $1 \times s$  matrix consists of polynomials in  $\widehat{\mathcal{L}}$  of degree  $s - 1$  (although typically not monic). Compared with stiffly accurate schemes, this now requires  $(s - 1)s$  matrix-vector multiplications, which is  $s - 1$  more than for stiffly accurate schemes, but still typically of marginal overall computational cost.

## 2.2 Preconditioning by conjugate pairs

Following the discussion and algorithm developed in Section 2.1, the key outstanding point is inverting  $\det(\mathcal{M}_s)^{-1}$ . Moving forward, we restrict our attention to the case  $\widehat{\mathcal{L}}_i = \widehat{\mathcal{L}}_j$  for all  $i, j$ , in which case we have a simple closed form for  $\det(\mathcal{M}_s)^{-1} = P_s(\widehat{\mathcal{L}})^{-1}$ , where  $P_s(x)$  is the characteristic polynomial of  $A_0^{-1}$  (see Lemma 1).

In contrast to much of the early work on solving IRK systems, where LU factorizations were the dominant cost and system sizes relatively small, explicitly forming and inverting  $P_s(\widehat{\mathcal{L}})$  for numerical PDEs is typically not a viable option in high-performance simulation on modern computing architectures. Instead, by computing the eigenvalues  $\{\lambda_i\}$  of  $A_0^{-1}$ , we can express  $P_s(\widehat{\mathcal{L}})$  in a factored form,

$$P_s(\widehat{\mathcal{L}}) = \prod_{i=1}^s (\lambda_i I - \widehat{\mathcal{L}}), \quad (10)$$

and its inverse can then be computed by successive applications of  $(\lambda_i I - \widehat{\mathcal{L}})^{-1}$ , for  $i = 1, \dots, s$ . Unfortunately, eigenvalues of  $A_0$  and  $A_0^{-1}$  are often complex, and

for real-valued matrices this makes the inverse of individual factors  $(\lambda_i I - \widehat{\mathcal{L}})^{-1}$  more difficult and often impractical with standard preconditioners and existing software. Moving forward, let  $\lambda := \eta + i\beta$  denote an eigenvalue of  $A_0^{-1}$ , for  $\eta, \beta \in \mathbb{R}$ , with  $\beta \geq 0$  and  $\eta > 0$  under ?? 1.

Here, we combine conjugate eigenvalues into quadratic polynomials that we must precondition, which take the form

$$\begin{aligned} \mathcal{Q}_\eta &:= ((\eta + i\beta)I - \widehat{\mathcal{L}})((\eta - i\beta)I - \widehat{\mathcal{L}}) \\ &= (\eta^2 + \beta^2)I - 2\eta\widehat{\mathcal{L}} + \widehat{\mathcal{L}}^2 = (\eta I - \widehat{\mathcal{L}})^2 + \beta^2 I. \end{aligned} \quad (11)$$

In practice, we typically do not want to directly form or precondition a quadratic operator like (11), due to (i) the overhead cost of large parallel matrix multiplication, and (ii) the fact that many fast parallel methods such as multigrid are not well-suited for solving a polynomial in  $\widehat{\mathcal{L}}$ . The point of (11) is that by considering conjugate pairs of eigenvalues, the resulting operator is real-valued. Here we propose preconditioning (11) with the inverse of a real-valued quadratic polynomial,  $(\delta I - \widehat{\mathcal{L}})(\gamma I - \widehat{\mathcal{L}})$ , for  $\delta, \gamma \in \mathbb{R}^+$ .

### 2.3 Optimal preconditioning

A natural starting point is preconditioning (11) with the inverse of the real-valued part of the operator,  $(\eta I - \widehat{\mathcal{L}})^2$ , dropping the  $+\beta^2 I$  term, which can be applied as two successive inverses of  $(\eta I - \widehat{\mathcal{L}})$ . Expanding, the preconditioned operator then takes the form

$$\begin{aligned} \mathcal{P}_\eta &:= (\eta I - \widehat{\mathcal{L}})^{-2} \left[ (\eta^2 + \beta^2)I - 2\eta\widehat{\mathcal{L}} + \widehat{\mathcal{L}}^2 \right] \\ &= I + \beta^2(\eta I - \widehat{\mathcal{L}})^{-2} = I + \frac{\beta^2}{\eta^2} \left( I - \frac{1}{\eta}\widehat{\mathcal{L}} \right)^{-2}. \end{aligned} \quad (12)$$

For  $\eta > \beta$  and under the assumptions introduced in Section 1.5, the preconditioned operator in (12) has a well bounded field-of-values, which can be directly translated into guaranteed GMRES convergence bounds [28]. However, for  $\beta \gg \eta$ , such a preconditioning is less effective.

Thus, consider a more general preconditioner of similar form, but with two separate constants  $\gamma, \delta > 0$ , where the preconditioned operator takes the form

$$\mathcal{P}_{\delta, \gamma} := (\delta I - \widehat{\mathcal{L}})^{-1}(\gamma I - \widehat{\mathcal{L}})^{-1} \left[ (\eta I - \widehat{\mathcal{L}})^2 + \beta^2 I \right]. \quad (13)$$

Such an approach was proven effective for symmetric definite spatial matrices in [5], where it is assumed  $\gamma = \delta$ , and the optimal constant is derived to be  $\gamma = \gamma_* = \sqrt{\eta^2 + \beta^2}$ . The following theorem derives tight bounds on the condition number of  $\mathcal{P}_{\delta, \gamma}$  (13), as well as optimality of  $\gamma \in (0, \infty)$ , in a much more general context. Corollary 1 then shows that the optimal preconditioner over all  $\delta, \gamma \in (0, \infty)$ , in terms of minimizing a tight upper bound on  $\ell^2$ -condition number, is given by

$$\mathcal{P}_{\gamma_*} := (\gamma_* I - \widehat{\mathcal{L}})^{-2} \left[ (\eta I - \widehat{\mathcal{L}})^2 + \beta^2 I \right]. \quad (14)$$

where  $\delta = \gamma = \gamma_* = \sqrt{\eta^2 + \beta^2}$ .

**Theorem 1** (Optimal preconditioning). *Suppose ?? 1?? 2 hold, that is,  $\eta > 0$  and  $W(\widehat{\mathcal{L}}) \leq 0$ , and suppose  $\widehat{\mathcal{L}}$  is real-valued. Let  $\mathcal{P}_{\delta,\gamma}$  denote the preconditioned operator as in (13), where  $[(\eta I - \widehat{\mathcal{L}})^2 + \beta^2 I]$  is preconditioned with  $(\delta I - \widehat{\mathcal{L}})^{-1}(\gamma I - \widehat{\mathcal{L}})^{-1}$ , for  $\delta, \gamma \in (0, \infty)$ . Let  $\kappa(\mathcal{P}_{\delta,\gamma})$  denote the two-norm condition number of  $\mathcal{P}_{\delta,\gamma}$ , and define  $\gamma_*$  by*

$$\gamma_* := \frac{\eta^2 + \beta^2}{\delta}. \quad (15)$$

Then

$$\kappa(\mathcal{P}_{\delta,\gamma_*}) \leq \frac{1}{2\eta} \left( \delta + \frac{\eta^2 + \beta^2}{\delta} \right). \quad (16)$$

Moreover, (i) bound (16) is tight in the sense that  $\exists \widehat{\mathcal{L}}$  such that (16) holds with equality, and (ii)  $\gamma = \gamma_*$  is optimal in the sense that, without further assumptions on  $\widehat{\mathcal{L}}$ ,  $\gamma_*$  minimizes a tight upper bound on  $\kappa(\mathcal{P}_{\delta,\gamma})$  over all  $\gamma \in (0, \infty)$ .

*Proof.* First we will prove bound (16), then we will demonstrate it is tight, and finally we will demonstrate the optimality of  $\gamma = \gamma_*$ .

The square of the condition number of  $\mathcal{P}_{\delta,\gamma}$  is given by

$$\kappa^2(\mathcal{P}_{\delta,\gamma}) = \|\mathcal{P}_{\delta,\gamma}\|^2 \|\mathcal{P}_{\delta,\gamma}^{-1}\|^2 = \max_{\mathbf{v} \neq 0} \frac{\|\mathcal{P}_{\delta,\gamma} \mathbf{v}\|^2}{\|\mathbf{v}\|^2} \frac{1}{\min_{\mathbf{v} \neq 0} \frac{\|\mathcal{P}_{\delta,\gamma} \mathbf{v}\|^2}{\|\mathbf{v}\|^2}}, \quad (17)$$

where for real-valued  $\widehat{\mathcal{L}}$ , the max and min can be obtained by restricting ourselves to real-valued  $\mathbf{v}$ . The key step in establishing (16) is bounding  $\|\mathcal{P}_{\delta,\gamma}\|^2$  and  $\|\mathcal{P}_{\delta,\gamma}^{-1}\|^2$  from above by bounding  $\|\mathcal{P}_{\delta,\gamma} \mathbf{v}\|^2 / \|\mathbf{v}\|^2$  from above and below, respectively. Consider the form of the preconditioned operator  $\mathcal{P}_{\delta,\gamma}$  in (13) and make the substitution  $\mathbf{v} \mapsto (\gamma I - \widehat{\mathcal{L}})(\delta I - \widehat{\mathcal{L}})\mathbf{w}$ . Using the fact that rational functions of  $\mathcal{L}$  commute,  $\|\mathcal{P}_{\delta,\gamma} \mathbf{v}\|^2$  can be expanded for real-valued  $\mathbf{v}$  (and, thus, real-valued  $\mathbf{w}$ ) as

$$\begin{aligned} \|\mathcal{P}_{\delta,\gamma} \mathbf{v}\|^2 &= \|[(\eta I - \widehat{\mathcal{L}})^2 + \beta^2] \mathbf{w}\|^2, \\ &= \|[(\eta^2 + \beta^2)\mathbf{w} - 2\eta \widehat{\mathcal{L}} \mathbf{w} + \widehat{\mathcal{L}}^2 \mathbf{w}]\|^2 \\ &= \|(\eta^2 + \beta^2)\mathbf{w} + \widehat{\mathcal{L}}^2 \mathbf{w}\|^2 - 4\eta(\eta^2 + \beta^2)\langle \widehat{\mathcal{L}} \mathbf{w}, \mathbf{w} \rangle \\ &\quad - 4\eta\langle \widehat{\mathcal{L}}(\widehat{\mathcal{L}} \mathbf{w}), \widehat{\mathcal{L}} \mathbf{w} \rangle + 4\eta^2 \|\widehat{\mathcal{L}} \mathbf{w}\|^2. \end{aligned} \quad (18)$$

Similarly, expanding  $\|\mathbf{v}\|^2$  yields

$$\begin{aligned} \|\mathbf{v}\|^2 &= \|(\gamma I - \widehat{\mathcal{L}})(\delta I - \widehat{\mathcal{L}})\mathbf{w}\|^2, \\ &= \|\delta\gamma \mathbf{w} - (\delta + \gamma)\widehat{\mathcal{L}} \mathbf{w} + \widehat{\mathcal{L}}^2 \mathbf{w}\|^2, \\ &= \|\delta\gamma \mathbf{w} + \widehat{\mathcal{L}}^2 \mathbf{w}\|^2 - 2\delta\gamma(\delta + \gamma)\langle \widehat{\mathcal{L}} \mathbf{w}, \mathbf{w} \rangle \\ &\quad - 2(\delta + \gamma)\langle \widehat{\mathcal{L}}(\widehat{\mathcal{L}} \mathbf{w}), \widehat{\mathcal{L}} \mathbf{w} \rangle + (\delta + \gamma)^2 \|\widehat{\mathcal{L}} \mathbf{w}\|^2. \end{aligned} \quad (19)$$

Thus, the key ratio in (17) takes the form

$$\frac{\|\mathcal{P}_{\delta,\gamma}\mathbf{v}\|^2}{\|\mathbf{v}\|^2} = \frac{c_0(\mathbf{w})f_0(\mathbf{w}) + c_1f_1(\mathbf{w}) + c_2f_2(\mathbf{w}) + c_3f_3(\mathbf{w})}{f_0(\mathbf{w}) + f_1(\mathbf{w}) + f_2(\mathbf{w}) + f_3(\mathbf{w})}, \quad (20)$$

where for  $\delta, \gamma > 0$ , we have defined the functions and constants

$$\begin{aligned} f_0 &:= \|\delta\gamma\mathbf{w} + \widehat{\mathcal{L}}^2\mathbf{w}\|^2 \geq 0, & c_0 &:= \frac{\|(\eta^2 + \beta^2)\mathbf{w} + \widehat{\mathcal{L}}^2\mathbf{w}\|^2}{\|\delta\gamma\mathbf{w} + \widehat{\mathcal{L}}^2\mathbf{w}\|^2} \geq 0, \\ f_1 &:= -2\delta\gamma(\delta + \gamma)\langle \widehat{\mathcal{L}}\mathbf{w}, \mathbf{w} \rangle \geq 0, & c_1 &:= \frac{\eta^2 + \beta^2}{\delta\gamma} \frac{2\eta}{\delta + \gamma} > 0, \\ f_2 &:= -2(\delta + \gamma)\langle \widehat{\mathcal{L}}(\widehat{\mathcal{L}}\mathbf{w}), \widehat{\mathcal{L}}\mathbf{w} \rangle \geq 0, & c_2 &:= \frac{2\eta}{\delta + \gamma} > 0, \\ f_3 &:= (\delta + \gamma)^2 \|\widehat{\mathcal{L}}\mathbf{w}\|^2 \geq 0, & c_3 &:= \left(\frac{2\eta}{\delta + \gamma}\right)^2 > 0. \end{aligned} \quad (21)$$

Note that functions  $f_1$  and  $f_2$  are non-negative by assumption of  $W(\widehat{\mathcal{L}}) \leq 0$ , while for all  $\mathbf{w} \neq \mathbf{0}$ , it must hold that either  $c_0f_0 > 0$  or  $c_3f_3 > 0$  (or both, because  $c_3f_3 = 0$  i.f.f.  $\widehat{\mathcal{L}}\mathbf{w} = \mathbf{0}$ , which implies  $c_0f_0 > 0$  for  $\mathbf{w} \neq \mathbf{0}$ ).

Since all of the addends in the numerator and denominator of (20) are non-negative, and at least one addend in each is positive, (20) can be bounded as

$$\min\{c_0, c_1, c_2, c_3\} =: c_{\min} \leq \frac{\|\mathcal{P}_{\delta,\gamma}\mathbf{v}\|^2}{\|\mathbf{v}\|^2} \leq c_{\max} := \max\{c_0, c_1, c_2, c_3\}.$$

Applying these bounds to the norms in (17) yields

$$\|\mathcal{P}_{\delta,\gamma}\| \leq \sqrt{c_{\max}}, \quad \|\mathcal{P}_{\delta,\gamma}^{-1}\| \leq \frac{1}{\sqrt{c_{\min}}}. \quad (22)$$

Bounding  $c_0$  for general  $\gamma$ , and hence  $c_{\min}$  and  $c_{\max}$ , is difficult because the sign of  $\langle \widehat{\mathcal{L}}^2\mathbf{w}, \mathbf{w} \rangle$  (which appears in expanding  $\|\delta\gamma\mathbf{w} + \widehat{\mathcal{L}}^2\mathbf{w}\|^2$ ) is not known for general  $\widehat{\mathcal{L}}$ , noting that the sign of  $W(\widehat{\mathcal{L}})$  does not determine that of  $W(\widehat{\mathcal{L}}^2)$ . However, observe from (21) that the judicious choice of  $\gamma = \gamma_* := (\eta^2 + \beta^2)/\delta$  yields  $c_0(\mathbf{w}) = 1$ . Moreover, in the final part of this proof we demonstrate that  $\gamma = \gamma_*$  is optimal, and, as such, moving forward we only consider the case  $\gamma = \gamma_*$ .

Letting  $\gamma = \gamma_* := (\eta^2 + \beta^2)/\delta$ , from (21) one has  $c_0 = 1 \geq c_1 = c_2 = \sqrt{c_3} = 2\eta/(\delta + \gamma_*)$ , where the inequality  $1 \geq 2\eta/(\delta + \gamma_*)$  follows by noting the equivalent relation  $\delta^2 - 2\eta\delta + \eta^2 + \beta^2 \geq 0$  for all  $\eta, \delta > 0$ . Thus, for  $\gamma = \gamma_*$ , the bounds in (22) are given by

$$\|\mathcal{P}_{\delta,\gamma_*}\| \leq 1, \quad \|\mathcal{P}_{\delta,\gamma_*}^{-1}\| \leq \frac{\delta + \gamma_*}{2\eta} = \frac{1}{2\eta} \left( \delta + \frac{\eta^2 + \beta^2}{\delta} \right) \quad (23)$$

Applying these bounds to the condition number (17) yields the upper bound in (16).

We now show that bound (16) is tight and that  $\gamma = \gamma_*$  is optimal. We do so by construction, showing that the bound in (16) is achieved for certain matrices, and that for  $\gamma \neq \gamma_*$ ,  $\exists$  matrices  $\widehat{\mathcal{L}}$  for which  $\kappa(\mathcal{P}_{\delta,\gamma}) > (\delta + \gamma_*)/(2\eta)$ . Note that

the min/max of  $\|\mathcal{P}_{\delta,\gamma}\mathbf{v}\|^2/\|\mathbf{v}\|^2$  over  $\mathbf{v}$  for real-valued  $\mathcal{P}_{\delta,\gamma}$  is equivalent when minimizing over real or complex  $\mathbf{v}$ ; we now consider complex  $\mathbf{v}$  for theoretical purposes. To that end, let  $\mathbf{v} = (\gamma I - \widehat{\mathcal{L}})(\delta I - \widehat{\mathcal{L}})\mathbf{w}$ , but suppose that  $(i\xi, \mathbf{w})$  is an eigenpair of  $\widehat{\mathcal{L}}$ , with  $\xi$  a real number and  $\mathbf{w}$  a complex eigenvector. Plugging into  $\|\mathcal{P}_{\delta,\gamma}\mathbf{v}\|^2$  (18) and  $\|\mathbf{v}\|^2$  (19), and taking the ratio as in (20), define the following function of  $\xi$ :

$$\mathcal{H}_{\delta,\gamma}(\xi) := \frac{\|\mathcal{P}_{\delta,\gamma}\mathbf{v}\|^2}{\|\mathbf{v}\|^2} \Big|_{\widehat{\mathcal{L}}\mathbf{w}=i\xi\mathbf{w}} = \frac{|\eta - i\xi|^2 + \beta^2}{|(\delta\gamma - \xi^2 - i(\delta + \gamma)\xi)|^2} = \frac{(\delta\gamma_* - \xi^2)^2 + (2\eta\xi)^2}{(\delta\gamma - \xi^2)^2 + [\xi(\delta + \gamma)]^2}, \quad (24)$$

where we have made use of  $\delta\gamma_* = \eta^2 + \beta^2$ . By virtue of restricting that  $\mathbf{w}$  be an eigenvector, from (17) we have

$$\frac{1}{\|\mathcal{P}_{\delta,\gamma}^{-1}\|^2} = \min_{\mathbf{v} \neq 0} \frac{\|\mathcal{P}_{\delta,\gamma}\mathbf{v}\|^2}{\|\mathbf{v}\|^2} \leq \mathcal{H}_{\delta,\gamma}(\xi) \leq \max_{\mathbf{v} \neq 0} \frac{\|\mathcal{P}_{\delta,\gamma}\mathbf{v}\|^2}{\|\mathbf{v}\|^2} = \|\mathcal{P}_{\delta,\gamma}\|^2. \quad (25)$$

That is, any value of  $1/\mathcal{H}_{\delta,\gamma}(\xi)$  serves as a lower bound on  $\|\mathcal{P}_{\delta,\gamma}^{-1}\|^2$ , while any value of  $\mathcal{H}_{\delta,\gamma}(\xi)$  serves as a lower bound on  $\|\mathcal{P}_{\delta,\gamma}\|^2$ . Therefore, the ratio of any two values of  $\mathcal{H}_{\delta,\gamma}(\xi)$  provides a lower bound on  $\kappa^2(\mathcal{P}_{\delta,\gamma})$ .

We now show that bound (16) on  $\kappa(\mathcal{P}_{\delta,\gamma_*})$  is tight. Considering (24) at the judiciously chosen eigenvalues of  $i\xi = \{0, \pm i\sqrt{\delta\gamma_*}\}$ , we have

$$\mathcal{H}_{\delta,\gamma}(0) = \frac{\gamma_*^2}{\gamma^2}, \quad \mathcal{H}_{\delta,\gamma}(\pm i\sqrt{\delta\gamma_*}) = \frac{(2\eta)^2\gamma_*}{\delta(\gamma - \gamma_*)^2 + \gamma_*(\delta + \gamma)^2}. \quad (26)$$

First observe from (25) and (26) that  $\|\mathcal{P}_{\delta,\gamma_*}\|^2 \geq \mathcal{H}_{\delta,\gamma_*}(0) = 1$ , and thus the upper bound on  $\|\mathcal{P}_{\delta,\gamma_*}\|$  from (23) achieves equality for a matrix  $\widehat{\mathcal{L}}$  having an eigenvalue of  $\xi = 0$ . Secondly, observe from (25) and (26) that  $\|\mathcal{P}_{\delta,\gamma_*}^{-1}\|^2 \geq 1/\mathcal{H}_{\delta,\gamma_*}(\pm i\sqrt{\delta\gamma_*}) = [(\delta + \gamma_*)/(2\eta)]^2$ , and thus the upper bound on  $\|\mathcal{P}_{\delta,\gamma_*}^{-1}\|$  from (23) achieves equality for a matrix  $\widehat{\mathcal{L}}$  having eigenvalues  $i\xi = \pm i\sqrt{\delta\gamma_*}$ . Therefore, bound (16) on  $\kappa(\mathcal{P}_{\delta,\gamma_*})$  achieves equality for any matrix  $\widehat{\mathcal{L}}$  having eigenvalues  $\{0, \pm i\sqrt{\delta\gamma_*}\}$ .<sup>4</sup>

Finally, having shown that (16) is tight, we now show that  $\gamma = \gamma_*$  is optimal. Once again, consider the matrix  $\widehat{\mathcal{L}}$  from above with eigenvalues  $\{0, \pm i\sqrt{\delta\gamma_*}\}$ , such that  $\kappa(\mathcal{P}_{\delta,\gamma_*}) = (\delta + \gamma_*)/(2\eta)$ . Now, observe from this, (25), and (26), that for  $0 < \gamma < \gamma_*$ ,

$$\kappa^2(\mathcal{P}_{\delta,\gamma_*}) < \frac{\gamma_*[\delta(\gamma - \gamma_*)^2 + \gamma_*(\delta + \gamma)^2]}{(2\eta\gamma)^2} = \frac{\mathcal{H}_{\delta,\gamma}(0)}{\mathcal{H}_{\delta,\gamma}(\pm i\sqrt{\delta\gamma_*})} \leq \kappa^2(\mathcal{P}_{\delta,\gamma}), \quad (27)$$

by noting that the first inequality in (27) is equivalent to  $\gamma_*(\gamma_* - \gamma)^2 + (\gamma_* - \gamma)[2\gamma_*\gamma + \delta(\gamma_* + \gamma)] > 0$ , which is clearly true when  $0 < \gamma < \gamma_*$ . Now suppose that  $\widehat{\mathcal{L}}$  has eigenvalues  $i\xi \rightarrow \pm i\infty$ , which, when substituted into (24), yields  $\lim_{\xi \rightarrow \pm\infty} \mathcal{H}_{\delta,\gamma}(\xi) = 1$ . Combining with (25) and (26), we have for  $\gamma_* < \gamma < \infty$ ,

$$\kappa^2(\mathcal{P}_{\delta,\gamma_*}) < \frac{\delta(\gamma - \gamma_*)^2 + \gamma_*(\delta + \gamma)^2}{(2\eta)^2\gamma_*} = \frac{\mathcal{H}_{\delta,\gamma}(\pm\infty)}{\mathcal{H}_{\delta,\gamma}(\pm i\sqrt{\delta\gamma_*})} \leq \kappa^2(\mathcal{P}_{\delta,\gamma}), \quad (28)$$

<sup>4</sup>By nature of the continuity of eigenvalues and continuity of  $\mathcal{H}_{\delta,\gamma}(\xi)$  at  $\xi = 0$ , there also exist nonsingular matrices with condition number within  $\epsilon$  of (16) for any  $\epsilon > 0$ .

by noting that the first inequality in (28) is equivalent to  $\delta(\gamma - \gamma_*)^2 + \gamma_*(\gamma - \gamma_*)(2\delta + \gamma_* + \gamma) > 0$ , which is clearly satisfied for  $\gamma > \gamma_*$ .

By construction in (27) and (28), we have shown that for all  $\gamma \in (0, \infty) \setminus \gamma_*$ , there exist matrices  $\widehat{\mathcal{L}}$  such that  $\kappa(\mathcal{P}_{\delta,\gamma}) > \kappa(\mathcal{P}_{\delta,\gamma_*}) = (\delta + \gamma_*)/(2\eta)$ . It therefore holds for general  $\widehat{\mathcal{L}}$  satisfying ?? 2 that a tight upper bound on  $\kappa(\mathcal{P}_{\delta,\gamma})$  for  $\gamma \in (0, \infty) \setminus \gamma_*$  must be larger than the tight upper bound of  $\kappa(\mathcal{P}_{\delta,\gamma_*}) \leq (\delta + \gamma_*)/(2\eta)$ . Hence  $\gamma = \gamma_*$  is the minimizer over  $\gamma \in (0, \infty)$  of a tight upper bound on  $\kappa(\mathcal{P}_{\delta,\gamma})$ .  $\square$

**Corollary 1** (Optimal preconditioning with  $\gamma = \delta$ ). *A tight upper bound on the condition number of the general operator  $\mathcal{P}_{\delta,\gamma}$  (13) is minimized over  $\delta, \gamma \in (0, \infty)$  when  $\delta = \gamma = \gamma_*$ , with*

$$\gamma_* = \sqrt{\eta^2 + \beta^2}. \quad (29)$$

*That is to say, the preconditioner  $(\gamma I - \widehat{\mathcal{L}})^{-2}$  employed in (14) with  $\gamma = \gamma_*$  is optimal over the space of general preconditioners  $(\delta I - \widehat{\mathcal{L}})^{-1}(\gamma I - \widehat{\mathcal{L}})^{-1}$ , for  $\delta, \gamma \in (0, \infty)$ . Furthermore, the condition number of the preconditioned operator  $\mathcal{P}_{\gamma_*}$  (14) is tightly bounded via*

$$\kappa(\mathcal{P}_{\gamma_*}) \leq \sqrt{1 + \frac{\beta^2}{\eta^2}}. \quad (30)$$

*Proof.* From Theorem 1, a tight upper bound on the condition number of  $\mathcal{P}_{\delta,\gamma}$  (13) is minimized with respect to  $\gamma$  when  $\gamma = \gamma_*$  (15), with its minimum value given by (16). To minimize bound (16) with respect to  $\delta$ , we differentiate it and observe for  $\delta > 0$  that there is only one critical point at  $\delta = \sqrt{\eta^2 + \beta^2}$ . Since this function is increasing as  $\delta \rightarrow 0^+$  and  $\delta \rightarrow \infty$ , this critical point must be a local minimum. Therefore, the tight upper bound (16) is minimized when  $\delta = \sqrt{\eta^2 + \beta^2}$ . Substituting  $\delta = \sqrt{\eta^2 + \beta^2}$  into (15) yields  $\gamma_* = \sqrt{\eta^2 + \beta^2}$ . Finally, substituting  $\delta = \gamma_* = \sqrt{\eta^2 + \beta^2}$  into (16) and noting that  $\mathcal{P}_{\gamma,\gamma}$  (13) is equivalent to  $\mathcal{P}_{\gamma}$  (14) yields bound (30).  $\square$

Table 1 provides condition number bounds from Corollary 1 and (30) for Gauss, Radau IIA, and Lobatto IIIC Runge-Kutta methods.

Stages	2		3		4		5		
	$\lambda_{1,2}^\pm$	$\lambda_1$	$\lambda_{2,3}^\pm$	$\lambda_{1,2}^\pm$	$\lambda_{3,4}^\pm$	$\lambda_1$	$\lambda_{2,3}^\pm$	$\lambda_{4,5}^\pm$	
Gauss	1.15	1.00	1.38	1.61	1.04	1.00	1.83	1.13	
Radau IIA	1.22	1.00	1.51	1.79	1.05	1.00	2.05	1.15	
Lobatto IIIC	1.41	1.00	1.79	2.12	1.06	1.00	2.42	1.17	

Table 1: Bounds on  $\kappa(\mathcal{P}_{\gamma_*})$  from Corollary 1 and (30) for Gauss, Radau IIA, and Lobatto IIIC integration, with 2–5 stages. Each column within a given set of stages corresponds to either a real eigenvalue,  $\lambda_1 = \eta$ , or a conjugate pair of eigenvalues, e.g.,  $\lambda_{2,3}^\pm = \eta \pm i\beta$ , of  $A_0^{-1}$ .

In the proof of Theorem 1,  $\gamma_*$  provides a delicate cancellation, and we have been unable to complete a general proof for  $\gamma \neq \gamma_*$  without further assumptions, such as  $W(\widehat{\mathcal{L}}^2) \geq 0$ . For the specific case of  $\delta = \gamma = \eta$ , one can derive a tight

bound of  $1 + \beta^2/\eta^2$  for SPD operators and  $\approx (1 + \beta^2/\eta^2)^{3/2}$  for skew symmetric operators (by appealing to normality). Numerical tests indicate using the modified constant  $\gamma_*$  as opposed to  $\eta$  is particularly important for hyperbolic-type problems. Indeed, one example in [Section 3.2](#) demonstrates an almost  $6\times$  reduction in iteration count achieved by using  $\gamma_*$  instead of  $\eta$ , whereas  $\gamma_*$  has offered a much more modest improvement over  $\eta$  for parabolic/diffusive problems we have explored. It is unclear if perhaps an  $\mathcal{O}(1)$  bound on condition number does not hold for general nonsymmetric operators with  $\delta = \gamma = \eta$ , or if the simple increase in condition number from  $\approx 1 + \beta^2/\eta^2 \mapsto (1 + \beta^2/\eta^2)^{3/2}$  is enough to cause a significant degradation in convergence. In any case,  $\mathcal{P}_{\gamma_*}$  has performed better than  $\mathcal{P}_\eta$  for all problems we have tested, and is the recommended preconditioner in practice.

**Remark 2** (Mass matrices). *Recall in the finite element context where mass matrices are involved, we defined  $\widehat{\mathcal{L}} := \delta t M^{-1} \mathcal{L}$ . For a given conjugate pair of eigenvalues, the quadratic polynomial (11) can be expressed as*

$$\mathcal{Q}_\eta = M^{-1}((\eta + i\beta)M - \delta t \mathcal{L})M^{-1}((\eta - i\beta)M - \delta t \widehat{\mathcal{L}}). \quad (31)$$

*In this context, it is best to first scale both sides of the linear system by  $M$ . This halves the number of times  $M^{-1}$  must be applied for each Krylov iteration, and if  $M$  and  $\mathcal{L}$  are Hermitian, the resulting quadratic system is SPD and can be solved using preconditioned CG or MINRES, preconditioned with one application of a preconditioner, the action of  $M$ , and a second application of the preconditioner.*

**Remark 3** (Inexact preconditioning). *In practice, fully converging  $(\gamma_* I - \widehat{\mathcal{L}})^{-1}$  each iteration as a preconditioner is often not desirable due to the cost of performing a full linear solve. Here, we propose applying a Krylov method to  $\mathcal{Q}_\eta := (\eta^2 + \beta^2)I - 2\eta\widehat{\mathcal{L}} + \widehat{\mathcal{L}}^2$  by computing the operator's action (that is, not fully constructing it), and preconditioning each Krylov iteration with two applications of a sparse parallel preconditioner for  $(\gamma_* I - \widehat{\mathcal{L}})$ , approximating the action of  $(\gamma_* I - \widehat{\mathcal{L}})^{-2}$ .*

*Analogous to standard block-preconditioning techniques, this approximate inverse approach is often (but not always) more efficient than computing a full inverse each iteration. However, it is important that the underlying preconditioner provides a good approximation. Fortunately, for difficult problems without highly effective preconditioners, it is straightforward to apply either multiple inner fixed-point iterations or an inner Krylov iteration (wrapped with a flexible outer Krylov method [36, 43]) to ensure robust (outer) iterations. In [Section 3.2.3](#), a numerical example is shown where the proposed method diverges using a single inner fixed-point iteration as a preconditioner for  $(\gamma_* I - \widehat{\mathcal{L}})$ , but three (or more) inner fixed-point iterations yields fast, scalable convergence.*

## 3 Numerical results

### 3.1 Finite-difference advection-diffusion

In this section, we consider a constant-coefficient advection-diffusion problem discretized in space with high-order finite-differences. An exact solution to this problem is used to demonstrate the high-order accuracy of the IRK methods,

and the robustness of the algorithms developed in the previous section with respect to mesh resolution. Specifically, we solve the PDE

$$u_t + 0.85u_x + u_y = 0.3u_{xx} + 0.25u_{yy} + s(x, y, t), \quad (x, y, t) \in (-1, 1)^2 \times (0, 2], \quad (32)$$

on a periodic spatial domain. The source term  $s(x, y, t)$  is chosen such that the solution of the PDE is  $u(x, y, t) = \sin^4(\pi/2[x - 1 - 0.85t]) \sin^4(\pi/2[y - 1 - t]) \exp(-[0.3 + 0.25]t)$ .

We consider tests using IRK methods of orders three, four, seven, and eight. The 3rd- and 4th-order IRK methods are paired with 4th-order central-finite-differences in space, and the 7th- and 8th-order methods with 8th-order central-finite-differences in space. In all cases, a time-step of  $\delta t = 2h$  is used, with  $h$  denoting the spatial mesh size, and results are run on four cores. Due to the diffusive, but non-SPD nature of the spatial discretization, we apply GMRES(30) preconditioned by a classical algebraic multigrid (AMG) method in the *hypre* library [15]. Specifically, we use classical interpolation (type 0), Falgout coarsening (type 6) with a strength tolerance  $\theta_C = 0.25$ , zero levels of aggressive coarsening, and  $L_1$ -Gauss-Seidel relaxation (type 8), with an absolute and relative stopping tolerance of  $10^{-13}$ . A single iteration of AMG is applied to approximate  $(\gamma_* I - \delta t \mathcal{L})^{-1}$ .

In [Figure 1](#), discretization errors are shown for different IRK methods, alongside the average number of AMG iterations needed per time step. The expected asymptotic convergence rates (black dashed lines in the left panel) are observed for all discretizations.<sup>5</sup>

The preconditioner appears robust with respect to mesh and problem size, since the average number of AMG iterations per time step (which is a proxy for the number of GMRES iterations) remains roughly constant as the mesh is refined. Of the fully implicit methods, the Gauss methods require the fewest AMG iterations, closely followed by Radau IIA methods, with the Lobatto IIIC methods requiring the most AMG iterations. This is consistent with the theoretical estimates in [Table 1](#). Note that while Gauss and Radau IIA methods have very similar iteration counts, Gauss converges at one order faster, which can be seen in the left-hand panel of the figure.

Considering the lower-order methods in the top row of [Figure 1](#), L-SDIRK(4), a 5-stage, 4th-order, L-stable SDIRK method requires the most AMG iterations of all methods. A-SDIRK(4), a 3-stage, 4th-order, A-stable SDIRK method, requires far fewer AMG iterations than L-SDIRK(4). However, A-SDIRK(4) yields a significantly larger discretization error than the other 4th-order schemes, and takes longer to reach its asymptotic convergence rate. Thus, in terms of work done per accuracy, the new preconditioner with 4th-order Gauss integration is the clear winner for this particular test problem, requiring roughly half the AMG iterations of the commonly used L-stable SDIRK4 scheme.

### 3.2 DG advection-diffusion

Here we consider a more difficult advection-diffusion problem, discretized using high-order DG finite elements. In particular, we demonstrate the effectiveness

<sup>5</sup>An exception here is A-SDIRK(4), which appears to be converging with a rate closer to three than four; however, further decreasing  $\delta t$  (not shown here) confirms 4th-order convergence is achieved eventually.

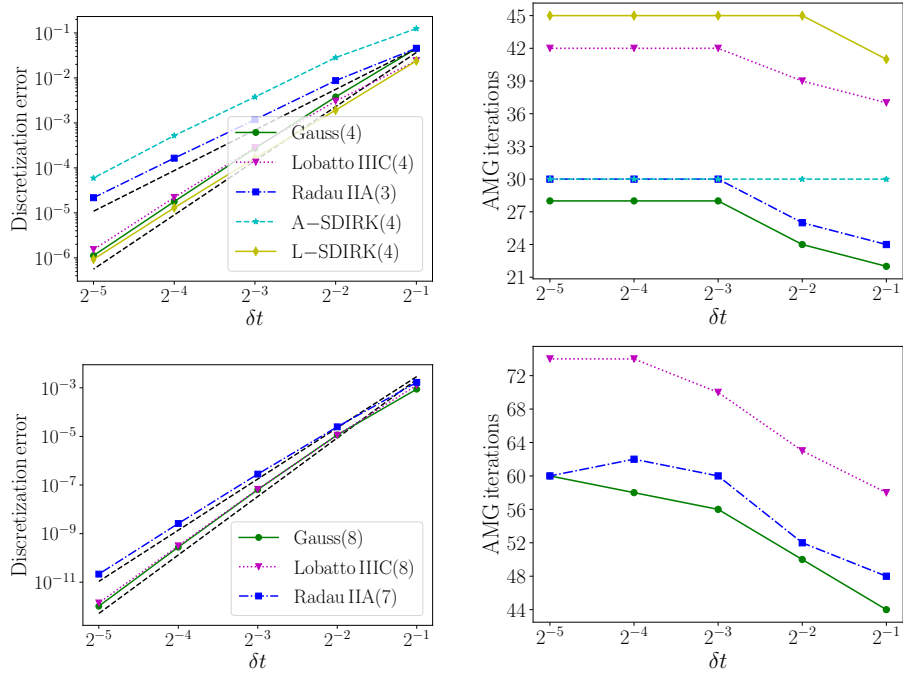


Figure 1: Finite-difference advection-diffusion problem (32).  $L_\infty$ -discretization errors at  $t = 2$  as a function of time-step  $\delta t$  are shown on the left for various discretizations of approximately 4th order (top) and 8th order (bottom). Black, dashed lines with slopes of three and four are shown (top), as are those with slopes of seven and eight (bottom). Plots on the right show the average number of AMG iterations per time step.

and scalability of the new preconditioning on more complex flows and DG discretizations (Figure 2 and Section 3.2.2), the reduction in computational work that can be achieved using large time steps and very high-order integration (Section 3.2.2), and how using multiple “inner” preconditioning iterations to approximate  $\widehat{\mathcal{L}}^{-1}$  (or even inner Krylov acceleration) can be important for the fast, scalable application of IRK integration (Section 3.2.3).

The governing equations in spatial domain  $\Omega = [0, 1] \times [0, 1]$  are given by

$$u_t + \nabla \cdot (\beta u - \varepsilon \nabla u) = f \quad (33)$$

where  $\beta(x, y) := (\cos(4\pi y), \sin(2\pi x))^T$  is the prescribed velocity field and  $\varepsilon$  the diffusion coefficient. Periodic boundary conditions are enforced on  $\partial\Omega$ , and (33) is discretized with an upwind DG method [14], where diffusion terms are treated with the symmetric interior penalty method [3, 4]. The resulting finite element problem is to find  $u_h \in V_h$  such that, for all  $v_h \in V_h$ ,

$$\begin{aligned} & \int_{\Omega} \partial_t(u_h) v_h \, dx - \int_{\Omega} u_h \beta \cdot \nabla_h v_h \, dx + \int_{\Gamma} \widehat{u}_h \beta \cdot \llbracket v_h \rrbracket \, ds + \int_{\Omega} \nabla_h u_h \cdot \nabla_h v_h \, dx \\ & - \int_{\Gamma} \{\nabla_h u_h\} \cdot \llbracket v_h \rrbracket \, ds - \int_{\Gamma} \{\nabla_h v_h\} \cdot \llbracket u_h \rrbracket \, ds + \int_{\Gamma} \sigma \llbracket u_h \rrbracket \cdot \llbracket v_h \rrbracket \, ds = \int_{\Omega} f v_h \, dx, \end{aligned}$$

where  $V_h$  is the DG finite element space consisting of piecewise polynomials of degree  $p$  defined on elements of the computational mesh  $\mathcal{T}$  of the spatial domain  $\Omega$ . No continuity is enforced between mesh elements. Here,  $\nabla_h$  is the broken gradient,  $\Gamma$  denotes the skeleton of the mesh, and  $\{\cdot\}$  and  $[[\cdot]]$  denote the average and jump of a function across a mesh interface.  $\widehat{u}_h$  is used to denote the upwind numerical flux. This discretization has been implemented in the MFEM finite element framework [2], and uses AMG preconditioning with approximate ideal restriction (AIR) [30, 31] (after first scaling by the inverse of the block-diagonal mass matrix).

The DG method is particularly well-suited for advection-dominated problems. In the following subsections we vary  $\varepsilon$  from 0 (purely advective) to 0.01. The velocity field, initial condition, and numerical solution for  $\varepsilon = 10^{-6}$  are shown in Figure 2.

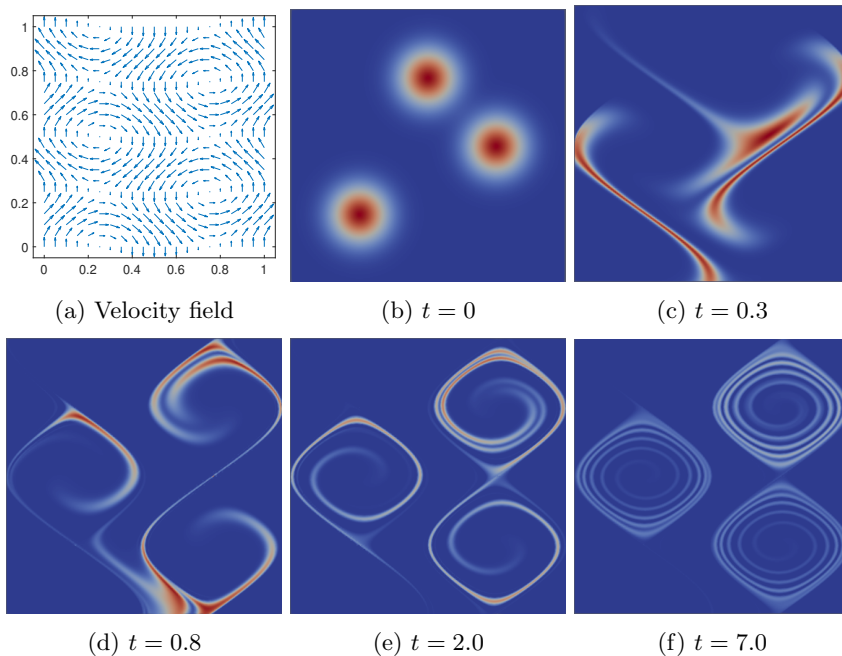


Figure 2: DG advection-diffusion problem with velocity field shown in subplot (a) and the solution plotted for various time points from  $t = 0$  to  $t = 7.0$  in subplots (b-f). Heatmap indicates solution in the 2d domain, with blue  $\mapsto 0$  and red  $\mapsto 1$ .

### 3.2.1 A hyperbolic example, and preconditioning with $\eta$ vs. $\gamma_*$

First, we demonstrate the effectiveness of using  $\gamma_*$  (Section 2.3) instead of  $\eta$  in the preconditioner, as well as the robustness of the proposed method on a fully hyperbolic problem, where most papers have only discussed parabolic PDEs. Thus, we set the diffusion coefficient  $\varepsilon = 0$  and apply AIR as a preconditioner for individual systems  $(\gamma M - \delta t \mathcal{L})$ .

AIR was originally designed for upwind DG discretizations of advection and is well-suited for this problem. We use the *hypre* implementation, with distance

1.5 restriction with strength tolerance  $\theta_R = 0.01$ , one-point interpolation (type 100), Falgout coarsening (type 6) with strength tolerance  $\theta_C = 0.1$ , no pre-relaxation, and forward Gauss Seidel post-relaxation (type 3), first on F-points followed by a second sweep on all points. The domain is discretized using 4th-order finite elements on a structured mesh, and the time step for each integration scheme is chosen such that the spatial and temporal orders of accuracy match; for example, for 8th-order integration we choose  $\delta t = \sqrt{h}$ , for mesh spacing  $h$ , so that  $\delta t^8 = h^4$ . All linear systems are solved to a relative tolerance of  $10^{-12}$ . There are a total of 1,638,400 spatial degrees-of-freedom (DOFs), and the simulations are run on 288 cores on the Quartz machine at Lawrence Livermore National Lab, resulting in  $\sim 5600$  DOFs/processor.

Table 2 shows the average number of AIR iterations to solve for each pair of stages of an IRK method using  $\eta$  and  $\gamma_*$  as the preconditioning constants. Iteration counts are shown for Gauss, Radau IIA, and Lobatto IIIC integration, with 2–5 stages, and the (factor of) reduction in iteration count achieved using  $\gamma_*$  vs.  $\eta$  is also shown. For 5-stage Lobatto IIIC integration,  $\gamma_*$  yields almost a  $6\times$  reduction in total inner AIR iterations to solve for the “hard” stage ( $\beta > \eta$ ), while in no cases is there an increase in iteration count when using  $\gamma_*$ .

Gauss								
Stages/Order	2/4	3/6		4/8		5/10		
Iterations( $\eta$ )	17	6	30	11	47	8	16	70
Iterations( $\gamma_*$ )	11	6	15	10	19	8	13	23
Speedup	1.5	1.0	2.0	1.1	2.5	1.0	1.2	3.0
Radau IIA								
Stages/Order	2/3	3/5		4/7		5/9		
Iterations( $\eta$ )	12	5	39	11	64	8	16	97
Iterations( $\gamma_*$ )	12	5	18	9	21	8	12	25
Speedup	1.0	1.0	2.2	1.2	3.0	1.0	1.3	3.9
Lobatto IIIC								
Stages/Order	2/2	3/4		4/6		5/8		
Iterations( $\eta$ )	8	3	67	11	113	7	17	175
Iterations( $\gamma_*$ )	8	3	22	9	26	7	12	30
Speedup	1.0	1.0	3.0	1.2	4.3	1.0	1.4	5.8

Table 2: Average AIR iterations to solve for each stage in an implicit Runge-Kutta method using preconditioners  $(\eta M - \delta t \mathcal{L})^{-2}$  and  $(\gamma_* M - \delta t \mathcal{L})^{-2}$ , with  $\gamma_*$  defined in (29). The ratio of iterations( $\eta$ )/iterations( $\gamma_*$ ) is shown in the “Speedup” rows.

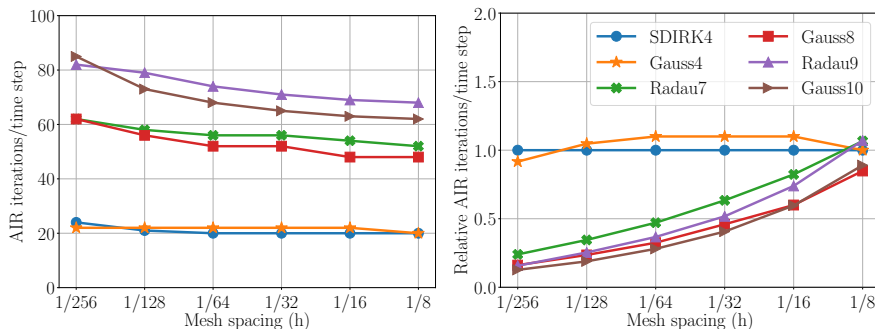
### 3.2.2 Advection-dominated

This section demonstrates high-order IRK integration applied to the advection-dominated problem in Figure 2, using AIR as a preconditioner for the linear systems.

Figure 3a shows the total number of AIR iterations required to compute

one time step using six different Runge-Kutta schemes, from 4th to 10th order, as a function of mesh spacing  $h$ . Note that as  $h \rightarrow 0$ , there is only modest growth in the number of AIR iterations per time step, indicating good (but not perfect) scalability. Moreover, note that there is small growth in the number of iterations for SDIRK4 as well (increasing from 20 to 25), which suggests the growth in iteration count is due to imperfect scalability of AIR iterations rather than the new IRK preconditioning.

Figure 3b then shows the relative number of AIR iterations to compute a given accuracy compared to SDIRK4. For example, if  $h = 0.01$ , then SDIRK4 uses  $\delta t_4 = 0.01$  and Gauss8 uses  $\delta t_8 = \sqrt{0.01} = 0.1 = 10\delta t_4$ , that is,  $10\times$  less time steps to achieve comparable accuracy. Note that as  $h \rightarrow 0$ , this factor becomes progressively larger. For quite moderate  $h$ , we see how very high-order integration can quickly lead to a reduction in total preconditioning iterations compared to a standard SDIRK4 scheme. Gauss8 and Radau9, for example, require almost  $7\times$  less AIR iterations than SDIRK4 at  $h = \delta t_4 = 1/256$ , and this ratio continues to decrease for smaller  $\delta t$ . Although this does not account for additional setup time, where Gauss8 and Radau9 require solving two and three different linear systems, respectively, and SDIRK4 only one, very high-order integration permitted through the new preconditioning still offers the opportunity for significant speedups.



(a) Total AIR iterations per time step (b) AIR iterations relative to SDIRK4

Figure 3

### 3.2.3 Diffusive problems and inner Krylov

In [30], AIR was shown to be effective on some DG advection-diffusion problems, and classical AMG is known to be effective on diffusion-dominated problems. However, the region of comparable levels of advection and diffusion remains the most difficult from a multigrid perspective. We use this to demonstrate how methods developed here require a “good” preconditioner for a backward Euler time step,  $(\gamma M - \delta t \mathcal{L})^{-1}$ , in order to converge on more general IRK methods. Fortunately, ensuring a preconditioner is sufficiently good can be resolved by appealing to standard block preconditioning techniques, where an inner iteration is used that applies multiple AIR iterations as a single preconditioner.

Here we consider an analogous problem to above, but set the diffusion coefficient to  $\varepsilon = 0.01$ . We use a mesh with spacing  $h \approx 0.001$ , 2nd-order DG finite elements, a time step of  $\delta t = 0.1$ , and three-stage 6th-order Gauss inte-

gration. Altogether, this yields equal orders of accuracy, with time and space error  $\sim 10^{-6}$ . FGMRES [43] is used for the outer iteration, which allows for GMRES to be applied in an inner iteration as a preconditioner for  $(\gamma_* M - \delta t \mathcal{L})$ . Figure 4 plots the total number of AIR iterations per time step as a function of the number of AIR iterations applied for each application of the preconditioner, using an inner GMRES or an inner fixed-point (Richardson) iteration. An advection-dominated problem with  $\varepsilon = 10^{-6}$  is also shown for comparison.

Recall we have three stages, one of which is a single linear system corresponding to a real eigenvalue, and the other corresponding to a pair of complex conjugate eigenvalues, which we precondition as in Section 2. The latter ends up being the more difficult problem to solve – for  $\varepsilon = 0.01$  (Figure 4b), the outer FGMRES iteration for the complex conjugate quadratic does not converge in 1000 iterations when using one AIR iteration as a preconditioner. If two AIR iterations with GMRES are used as a preconditioner, the FGMRES iteration converges in approximately 130 iterations, each of which requires two applications of GMRES preconditioned with two AIR iterations, yielding just over 500 total AIR iterations to converge. Further increasing the number of AIR iterations per preconditioning yields nice convergence using inner fixed-point or GMRES, with 150 and 112 total AIR iterations per time step, respectively. In contrast, Figure 4a shows that additional AIR iterations for the advection-dominated case are generally detrimental to overall computational cost (although the outer iteration converges slightly faster, it does not make up for the additional linear solves/iteration).

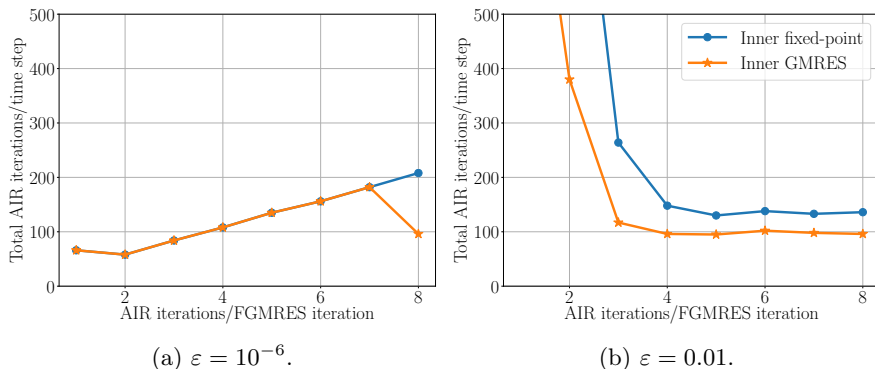


Figure 4: AIR iterations per time step as a function of the number of AIR iterations applied in each application of the preconditioner, for diffusion coefficient  $\varepsilon$ .

### 3.3 High-order matrix-free diffusion

In this example, we illustrate the use of high-order IRK methods coupled with high-order finite element spatial discretizations. It is well-known that matrix assembly becomes prohibitively expensive for high-order finite elements. Naive algorithms typically require  $\mathcal{O}(p^{3d})$  operations to assemble the resulting system matrix, where  $p$  is the polynomial degree and  $d$  is the spatial dimension. Techniques such as sum factorization can reduce this cost on tensor-product elements to  $\mathcal{O}(p^{2d+1})$ , however this cost can still be prohibitive for large values of  $p$  [33].

On the other hand, matrix-free operator evaluation on tensor-product meshes can be performed in  $\mathcal{O}(p^{d+1})$  operations [38], motivating the development of solvers and preconditioners that can be constructed and applied without access to the assembled system matrix [24].

We consider a high-order finite element discretization of the linear heat equation on spatial domain  $\Omega$ ,

$$\int_{\Omega} \partial_t(u_h)v_h \, dx + \int_{\Omega} \nabla u_h \cdot \nabla v_h \, dx = \int_{\Omega} f v_h \, dx,$$

where  $u_h, v_h \in V_h$ , and  $V_h$  denotes the degree- $p$   $H^1$ -conforming finite element space defined on a mesh  $\mathcal{T}$  consisting of tensor-product elements (i.e. quadrilaterals or hexahedra). The matrix-free action of the corresponding operator is computed in  $\mathcal{O}(p^{d+1})$  operations using the *partial assembly* features of the MFEM finite element library [2]. In order to precondition the resulting system, we make use of a low-order refined preconditioner, whereby the high-order system is preconditioned using a spectrally equivalent low-order finite element discretization computed on a refined mesh [11]. The low-order refined discretization can be assembled in  $\mathcal{O}(p^d)$  time, thereby avoiding the prohibitive costs of high-order matrix assembly. We make use of the uniform preconditioners for the low-order refined problem based on subspace corrections, developed in [39].

For this test case, take the spatial domain to be  $\Omega = [0, 1] \times [0, 1]$ , with periodic boundary conditions. We choose the forcing term

$$f(x, y, t) = \sin(2\pi x) \cos(2\pi y) (\cos(t) + 8\pi^2(2 + \sin(t))),$$

which corresponds to the exact solution

$$u(x, y, t) = \sin(2\pi x) \cos(2\pi y)(2 + \sin(t)).$$

We begin with a very coarse  $3 \times 3$  mesh, and integrate in time until  $t = 0.1$  using the Gauss and Radau IIA methods of orders 2 through 10. For each test case, the finite element polynomial degree is set to  $k - 1$ , where  $k$  is the order of accuracy of the time integration method, resulting in  $k$ th order convergence in both space and time. The mesh and time step are refined by factors of two to confirm the high-order convergence in space and time of the method. The relative  $L^2$  error, obtained by comparing against the exact solution, is shown in Figure 5.

We also use this test case to study the effect of inner iterations on the convergence of the iteration solver. As discussed in Remark 3, it is important that the underlying preconditioner provides a good approximation of the inverse of the operator. For that reason, we consider the use of an inner Krylov solver at every iteration. Since this corresponds to using a variable preconditioner at each iteration, a flexible Krylov method may have to be used for the outer iteration, although in practice good convergence is often still observed using the standard CG method [36]. In particular, we compare the total number of preconditioner applications required to converge the outer iteration to a relative tolerance of  $10^{-10}$ , both with and without an inner Krylov solver. For the inner Krylov solver, we use a CG iteration with the same relative tolerance as the outer iteration in order to give a good approximation to the inverse of the operator. The iteration counts are displayed in Figure 6. We note that for the

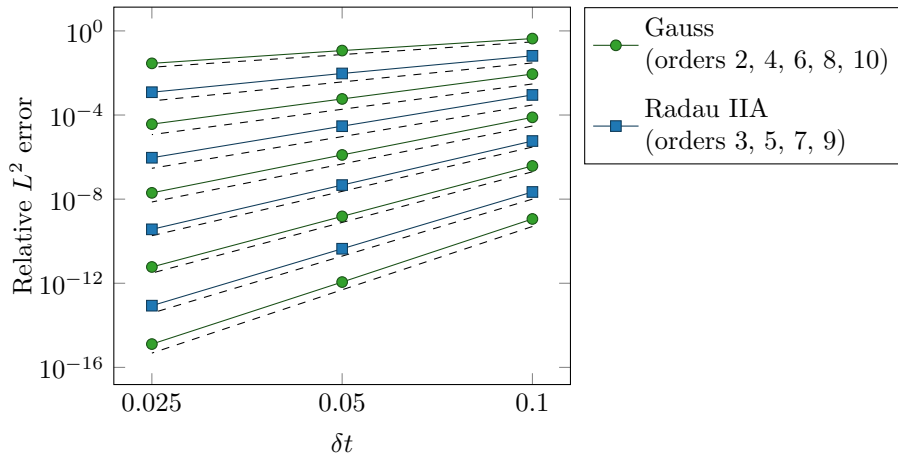


Figure 5: High-order convergence in space and time for the matrix-free diffusion problem. Gauss and Radau IIA methods of orders 2 through 10 are used. The dashed lines indicate the expected rates of convergence for each method.

fully implicit IRK methods, using an inner Krylov solver can reduce the total number of preconditioner applications by about a factor of 1.5, although this depends on the type of method and order of accuracy. As expected, the use of inner iterations does not reduce the total number of preconditioner applications for DIRK methods. In addition, for this test case, the total number of preconditioner applications required for the second and fourth order Gauss IRK methods is between 1.3 and 2 times smaller than those required for the corresponding equal-order DIRK methods.

## 4 Conclusions

This paper introduces a theoretical and algorithmic framework for the fast, parallel solution of fully implicit Runge-Kutta and DG discretizations in time for linear numerical PDEs. Theory is developed to guarantee  $\mathcal{O}(1)$  conditioning under general assumptions on the spatial discretization that yield stable time integration. Numerical results demonstrate the new method on various high-order finite-difference and finite-element discretizations of linear parabolic and hyperbolic problems, demonstrating fast, scalable solution of up to 10th order accuracy. In several cases, the new method can achieve 4th-order accuracy using Gauss integration with roughly half the number of preconditioner applications as required using standard SDIRK techniques. Ongoing work involves addressing fully nonlinear problems and algebraic constraints, in particular, without assuming that the linear system (3) can be expressed in Kronecker-product form (thus allowing for a true Newton or better Newton-like method compared with the commonly used/analyzed simplified Newton approach).

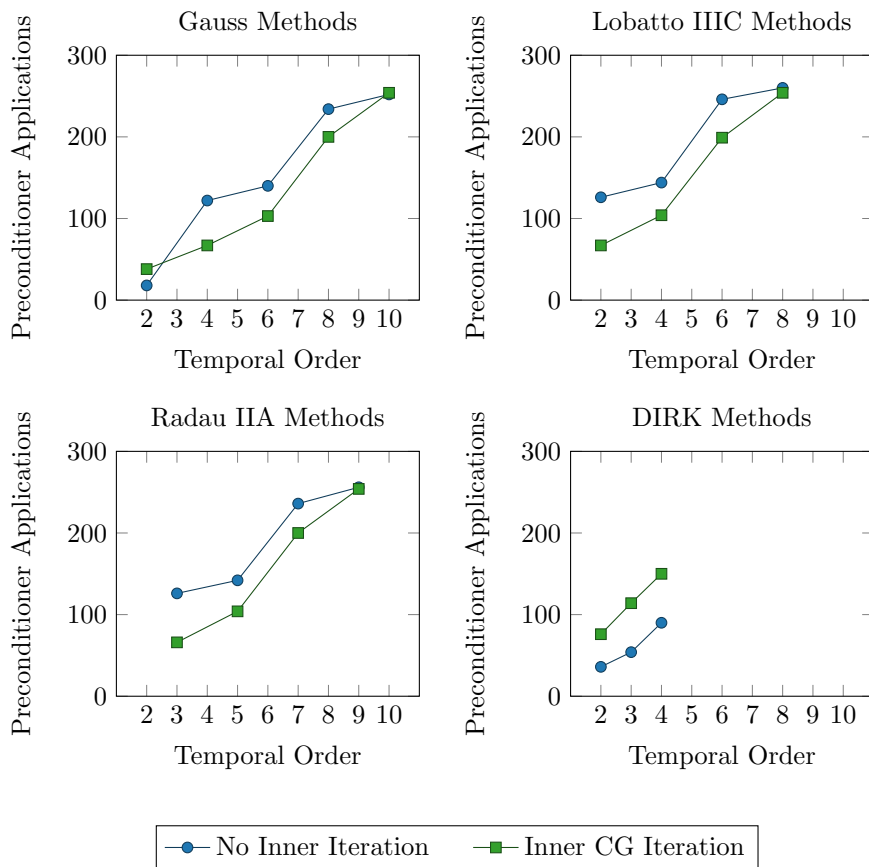


Figure 6: Comparison of total number of preconditioner applications with and without inner iterations. Both the outer iteration and the inner CG iteration are converged to a relative tolerance of  $10^{-10}$ .

## Acknowledgments

This work was performed under the auspices of the U.S. Department of Energy by Lawrence Livermore National Laboratory under Contract DE-AC52-07NA27344 (LLNL-JRNL-817946). Los Alamos National Laboratory report number LA-UR-20-30412. This document was prepared as an account of work sponsored by an agency of the United States government. Neither the United States government nor Lawrence Livermore National Security, LLC, nor any of their employees makes any warranty, expressed or implied, or assumes any legal liability or responsibility for the accuracy, completeness, or usefulness of any information, apparatus, product, or process disclosed, or represents that its use would not infringe privately owned rights. Reference herein to any specific commercial product, process, or service by trade name, trademark, manufacturer, or otherwise does not necessarily constitute or imply its endorsement, recommendation, or favoring by the United States government or Lawrence Livermore National Security, LLC. The views and opinions of authors expressed herein do not necessarily state or reflect those of the United States government or

Lawrence Livermore National Security, LLC, and shall not be used for advertising or product endorsement purposes.

## References

- [1] G. AKRIVIS, C. MAKRIDAKIS, AND R. H. NOCHETTO, *Galerkin and Runge-Kutta methods: unified formulation, a posteriori error estimates and nodal superconvergence*, *Numerische Mathematik*, 118 (2011), pp. 429–456, doi:10.1007/s00211-011-0363-6.
- [2] R. ANDERSON, J. ANDREJ, A. BARKER, J. BRAMWELL, J.-S. CAMIER, J. CERVENY, V. DOBREV, Y. DUDOUT, A. FISHER, T. KOLEV, W. PAZNER, M. STOWELL, V. TOMOV, J. DAHM, D. MEDINA, AND S. ZAMPINI, *MFEM: a modular finite element methods library*, *Computers & Mathematics with Applications*, (2020), doi:10.1016/j.camwa.2020.06.009.
- [3] D. N. ARNOLD, *An interior penalty finite element method with discontinuous elements*, *SIAM Journal on Numerical Analysis*, 19 (1982), pp. 742–760, doi:10.1137/0719052.
- [4] D. N. ARNOLD, F. BREZZI, B. COCKBURN, AND L. D. MARINI, *Unified analysis of discontinuous Galerkin methods for elliptic problems*, *SIAM Journal on Numerical Analysis*, 39 (2002), pp. 1749–1779, doi:10.1137/S0036142901384162.
- [5] S. BASTING AND E. BÄNSCH, *Preconditioners for the Discontinuous Galerkin time-stepping method of arbitrary order*, *ESAIM: Mathematical Modelling and Numerical Analysis*, 51 (2017), pp. 1173–1195, doi:10.1051/m2an/2016055.
- [6] T. A. BICKART, *An Efficient Solution Process for Implicit Runge–Kutta Methods*, *SIAM Journal on Numerical Analysis*, 14 (1977), pp. 1022–1027, doi:10.1137/0714069.
- [7] W. C. BROWN, *Matrices over commutative rings*, Marcel Dekker, Inc., 1993.
- [8] K. BURRAGE, *Efficiently Implementable Algebraically Stable Runge–Kutta Methods*, *SIAM Journal on Numerical Analysis*, 19 (1982), pp. 245–258, doi:10.1137/0719015.
- [9] J. BUTCHER AND D. CHEN, *A new type of singly-implicit Runge–Kutta method*, *Applied Numerical Mathematics*, 34 (2000), pp. 179–188, doi:10.1016/s0168-9274(99)00126-9.
- [10] J. C. BUTCHER, *On the implementation of implicit Runge-Kutta methods*, *BIT Numerical Mathematics*, 16 (1976), pp. 237–240, doi:10.1007/bf01932265.
- [11] C. CANUTO, P. GERVASIO, AND A. QUARTERONI, *Finite-element preconditioning of G-NI spectral methods*, *SIAM Journal on Scientific Computing*, 31 (2010), pp. 4422–4451, doi:10.1137/090746367.

- [12] H. CHEN, *A splitting preconditioner for the iterative solution of implicit Runge-Kutta and boundary value methods*, BIT Numerical Mathematics, 54 (2014), pp. 607–621, doi:10.1007/s10543-014-0467-3.
- [13] H. CHEN, *Kronecker product splitting preconditioners for implicit Runge-Kutta discretizations of viscous wave equations*, Applied Mathematical Modelling, 40 (2016), pp. 4429–4440, doi:10.1016/j.apm.2015.11.037.
- [14] B. COCKBURN AND C.-W. SHU, *Runge-Kutta discontinuous Galerkin methods for convection-dominated problems*, Journal of Scientific Computing, 16 (2001), pp. 173–261, doi:10.1023/a:1012873910884.
- [15] R. D. FALGOUT AND U. M. YANG, *hypre: A library of high performance preconditioners*, European Conference on Parallel Processing, 2331 LNCS (2002), pp. 632–641.
- [16] M. J. GANDER AND M. NEUMULLER, *Analysis of a new space-time parallel multigrid algorithm for parabolic problems*, SIAM Journal on Scientific Computing, 38 (2016), pp. A2173–A2208.
- [17] E. HAIRER AND G. WANNER, *Solving Ordinary Differential Equations II, Stiff and Differential-Algebraic Problems*, (1996), pp. 118–130, doi:10.1007/978-3-642-05221-7\_8.
- [18] E. HAIRER, G. WANNER, AND C. LUBICH, *Geometric Numerical Integration, Structure-Preserving Algorithms for Ordinary Differential Equations*, (2002), doi:10.1007/978-3-662-05018-7.
- [19] W. HOFFMANN AND J. J. B. D. SWART, *Approximating Runge-Kutta matrices by triangular matrices*, BIT Numerical Mathematics, 37 (1997), pp. 346–354, doi:10.1007/bf02510217.
- [20] P. J. V. D. HOUWEN AND J. J. B. D. SWART, *Parallel linear system solvers for Runge-Kutta methods*, Advances in Computational Mathematics, 7 (1997), pp. 157–181, doi:10.1023/a:1018990601750.
- [21] P. J. V. D. HOUWEN AND J. J. B. D. SWART, *Triangularly Implicit Iteration Methods for ODE-IVP Solvers*, SIAM Journal on Scientific Computing, 18 (1997), pp. 41–55, doi:10.1137/s1064827595287456.
- [22] L. O. JAY, *Inexact Simplified Newton Iterations for Implicit Runge-Kutta Methods*, SIAM Journal on Numerical Analysis, 38 (2000), pp. 1369–1388, doi:10.1137/s0036142999360573.
- [23] C. KENNEDY AND M. H. CARPENTER, *Diagonally Implicit Runge-Kutta Methods for Ordinary Differential Equations. A Review*, tech. report, 2016.
- [24] M. KRONBICHLER AND K. LJUNGKVIST, *Multigrid for matrix-free high-order finite element computations on graphics processors*, ACM Transactions on Parallel Computing, 6 (2019), pp. 1–32, doi:10.1145/3322813.
- [25] P. LASAINT AND P. RAVIART, *On a finite element method for solving the neutron transport equation*, Mathematical Aspects of Finite Elements in Partial Differential Equations, (1974), pp. 89–123, doi:10.1016/b978-0-12-208350-1.50008-x.

- [26] J. V. LENT AND S. VANDEWALLE, *Multigrid Methods for Implicit Runge–Kutta and Boundary Value Method Discretizations of Parabolic PDEs*, SIAM Journal on Scientific Computing, 27 (2005), pp. 67–92, doi:10.1137/030601144.
- [27] R. J. LEVEQUE, *Finite Difference Methods for Ordinary and Partial Differential Equations: Steady-State and Time-Dependent Problems*, vol. 98, Siam, 2007.
- [28] J. LIESEN AND P. TICHÝ, *The field of values bound on ideal GMRES*, arXiv preprint arXiv:1211.5969, (2020).
- [29] C. MAKRIDAKIS AND R. H. NOCHETTO, *A posteriori error analysis for higher order dissipative methods for evolution problems*, Numerische Mathematik, 104 (2006), pp. 489–514, doi:10.1007/s00211-006-0013-6.
- [30] T. A. MANTEUFFEL, S. MÜNZENMAIER, J. RUGE, AND B. S. SOUTHWORTH, *Nonsymmetric reduction-based algebraic multigrid*, SIAM J. Sci. Comput., 41 (2019), pp. S242–S268, doi:10.1137/18M1193761.
- [31] T. A. MANTEUFFEL, J. RUGE, AND B. S. SOUTHWORTH, *Nonsymmetric algebraic multigrid based on local approximate ideal restriction ( $\ell$ AIR)*, SIAM J. Sci. Comput., 40 (2018), pp. A4105–A4130, doi:10.1137/17M1144350.
- [32] K. A. MARDAL, T. K. NILSEN, AND G. A. STAFF, *Order-Optimal Preconditioners for Implicit Runge–Kutta Schemes Applied to Parabolic PDEs*, SIAM Journal on Scientific Computing, 29 (2007), pp. 361–375, doi:10.1137/05064093x.
- [33] J. MELENK, K. GERDES, AND C. SCHWAB, *Fully discrete hp-finite elements: fast quadrature*, Computer Methods in Applied Mechanics and Engineering, 190 (2001), pp. 4339–4364, doi:10.1016/s0045-7825(00)00322-4.
- [34] T. K. NILSEN, G. A. STAFF, AND K. MARDAL, *Order optimal preconditioners for fully implicit Runge-Kutta schemes applied to the bidomain equations*, Numerical Methods for Partial Differential Equations, 27 (2011), pp. 1290–1312, doi:10.1002/num.20582.
- [35] S. P. NØRSETT, *Runge-kutta methods with a multiple real eigenvalue only*, BIT Numerical Mathematics, 16 (1976), pp. 388–393.
- [36] Y. NOTAY, *Flexible conjugate gradients*, SIAM Journal on Scientific Computing, 22 (2000), pp. 1444–1460, doi:10.1137/s1064827599362314, <https://doi.org/10.1137%2Fs1064827599362314>.
- [37] B. OREL, *Real pole approximations to the exponential function*, BIT, 31 (1991), pp. 144–159, doi:10.1007/bf01952790.
- [38] S. A. ORSZAG, *Spectral methods for problems in complex geometries*, Journal of Computational Physics, 37 (1980), pp. 70–92, doi:10.1016/0021-9991(80)90005-4.

- [39] W. PAZNER, *Efficient low-order refined preconditioners for high-order matrix-free continuous and discontinuous Galerkin methods*, SIAM Journal on Scientific Computing (In Press), (2020).
- [40] W. PAZNER AND P.-O. PERSSON, *Stage-parallel fully implicit Runge–Kutta solvers for discontinuous Galerkin fluid simulations*, Journal of Computational Physics, 335 (2017), pp. 700–717, doi:10.1016/j.jcp.2017.01.050.
- [41] S. C. REDDY AND L. N. TREFETHEN, *Stability of the method of lines*, Numerische Mathematik, 62 (1992), pp. 235–267, doi:10.1007/bf01396228.
- [42] T. RICHTER, A. SPRINGER, AND B. VEXLER, *Efficient numerical realization of discontinuous Galerkin methods for temporal discretization of parabolic problems*, Numerische Mathematik, 124 (2013), pp. 151–182, doi:10.1007/s00211-012-0511-7.
- [43] Y. SAAD, *A flexible inner-outer preconditioned GMRES algorithm*, SIAM Journal on Scientific Computing, 14 (1993), pp. 461–469.
- [44] D. SCHÖTZAU AND C. SCHWAB, *Time Discretization of Parabolic Problems by the HP-Version of the Discontinuous Galerkin Finite Element Method*, SIAM Journal on Numerical Analysis, 38 (2000), pp. 837–875, doi:10.1137/s0036142999352394.
- [45] I. SMEARS, *Robust and efficient preconditioners for the discontinuous Galerkin time-stepping method*, IMA Journal of Numerical Analysis, (2016), p. drw050, doi:10.1093/imanum/drw050.
- [46] B. S. SOUTHWORTH, O. A. KRZYSIK, AND W. PAZNER, *Fast parallel solution of fully implicit Runge-Kutta and discontinuous Galerkin in time for numerical PDEs, part II: nonlinearities and DAEs*, arXiv preprint arXiv:TODO, (2020).
- [47] G. A. STAFF, K.-A. MARDAL, AND T. K. NILSSEN, *Preconditioning of fully implicit Runge-Kutta schemes for parabolic PDEs*, Modeling, Identification and Control: A Norwegian Research Bulletin, 27 (2006), pp. 109–123, doi:10.4173/mic.2006.2.3.
- [48] L. N. TREFETHEN AND M. EMBREE, *Spectra and pseudospectra: the behavior of nonnormal matrices and operators*, Princeton University Press, 2005.